

VAPOR PRESSURE LOWERING EFFECTS DUE TO SALINITY AND SUCTION PRESSURE IN THE DEPLETION OF VAPOR-DOMINATED GEOTHERMAL RESERVOIRS

Alfredo Bartistelli (+), Claudio Calore (*) and Karsten Pruess (&)

(+) Aquatec S.p.A., Via Miralbello 53, 61047 S. Lorenzo in Campo (PS), Italy.

(*) Istituto Internazionale per le Ricerche Geotermiche - CNR, Piazza Solferino 2, 56126 Pisa, Italy.

(&) Earth Sciences Division, Lawrence Berkeley Laboratory, 1 Cyclotron Road, Berkeley, CA 94720, USA.

Key words: numerical simulation, suction pressure, salt effects, permeability reduction, fractured reservoirs.

ABSTRACT

The equation-of-state module able to handle saline brines with non-condensable gas, developed for the TOUGH2 simulator, has been improved to include vapor pressure lowering (VPL) due to suction pressure as represented by Kelvin's equation. In this equation the effects of salt are considered whereas those of non-condensable gas have currently been neglected.

Numerical simulations of fluid production from tight matrix blocks have been performed to evaluate the impact of VPL effects due to salinity and suction pressure on the depletion behaviour of vapor-dominated geothermal reservoirs.

Previous studies performed neglecting VPL due to suction pressure showed that for initial NaCl mass fractions above threshold values, "sealing" of the block occurs and large amounts of liquid fluid may not be recovered. On the other hand, below the threshold value the matrix block dries out due to fluid production.

The inclusion of VPL due to suction pressure does not allow complete vaporization of the liquid phase. As a result, the threshold NaCl concentration above which sealing of the matrix block occurs is increased. Above the 'critical' NaCl concentration, block depletion behaviour with and without the VPL due to suction pressure is almost identical, as liquid phase saturation remains high even after long production times.

As the VPL due to suction pressure depends mainly on capillary pressure, the shape of capillary pressure functions used in numerical simulations is important in determining VPL effects on block depletion.

INTRODUCTION

An equation-of-state (EOS) module, here referred to as EWASG, able to handle saline brines with non-condensable gas (NCG), was developed by Bartistelli et al. (1993) for the TOUGH2 simulator. Vapor pressure lowering phenomena due to salinity only were considered in that EOS module version.

Capillary pressure and vapor adsorption effects, here referred to as suction pressure effects, and associated VPL phenomena are believed to have a large importance in determining the in-place and extractable fluid reserves of a geothermal reservoir (Nghiem and Ramey, 1991).

Modeling studies of the effects of capillarity and vapor adsorption on the depletion of vapor-dominated geothermal reservoirs have been performed by Pruess and O'Sullivan (1992) considering pure water. The VPL due to suction pressure has now been implemented in the EWASG module.

This paper illustrates the method used to model the VPL due to suction pressure in the presence of saline brines. We also present and discuss preliminary results of numerical simulations performed to evaluate the impact of these effects on the depletion of geothermal reservoirs containing saline brines. In these simulation studies the presence of NCG has not been accounted for.

MODELLING APPROACH

In the EWASG formulation the multiphase mixture is assumed to be composed of three mass components: water, sodium chloride and NCG. While water and NCG components may be present only in the liquid and gas phases, the salt component could be present dissolved in the liquid phase or precipitated to form a solid salt phase. The small solubility of NaCl in the gas phase is disregarded.

The reduction of rock porosity owing to salt precipitation is taken into account, as well as the related decrease of formation permeability according to the Verma and Pruess model (1988).

The dependence of brine enthalpy, density, viscosity and vapor pressure on salt concentration has been accounted for, as well as the effect on NCG solubility and heat of solution in the brine. Transport of the mass components occurs by advection in liquid and gas phases; binary diffusion in the gas phase for steam and the NCG is accounted for. Dispersive processes

in the liquid and gas phases are not included in the present formulation. It is assumed that the three phases (gas, liquid, and solid salt) are in local chemical and thermal equilibrium and that no chemical reactions take place other than interphase mass transfer.

In the integral finite differences formulation used by TOUGH2, the mass balance equations are written in the following general form (Pruess, 1991):

$$\frac{d}{dt} \int_{V_n} M^{(k)} dV = \int_{\Gamma_n} F^{(k)} \cdot \mathbf{n} d\Gamma + \int_{V_n} Q^{(k)} dV \quad (1)$$

where $k=1,2,3$ in EWASG indicates water, NaCl and NCG components, respectively. A complete description of the nomenclature used is given at the end of the paper. The accumulation and mass flux terms for the NaCl component ($k=2$) are written as follows:

$$M^{(2)} = \phi S_s \rho_s + \phi S_l \rho_l X_1^{(2)} \quad (2)$$

$$F^{(2)} = -k \frac{k_H}{\mu_1} \rho_l X_1^{(2)} (\text{grad} P_1 - \rho_l \mathbf{g}) \quad (3)$$

where S_s is the "solid saturation", defined as the fraction of pore volume occupied by solid salt.

The vapor pressure as affected by suction pressure and salinity effects is given by:

$$P_v(T, S_{la}, X_1^{(2)}) = f_{vPL}(T, S_{la}, X_1^{(2)}) P_{b, \text{sat}}(T, X_1^{(2)}) \quad (4)$$

where $P_{b, \text{sat}}$ is the saturated vapor pressure of brine with dissolved salt mass fraction $X_1^{(2)}$ at temperature T , and f_{vPL} is the vapor pressure lowering factor given by Kelvin's equation:

$$f_{vPL} = \left[\frac{W^{(1)} P_c(S_{la})}{\rho_l(P_1, T, X_1^{(2)}) R (T+273.15)} \right] \quad (5)$$

The capillary pressure is evaluated considering the 'active liquid phase' S_{la} . Active saturation of flowing phases is defined as:

$$S_{\beta a} = S_{\beta} / (1 - S_s) \quad (6)$$

where $\beta=l,g$ and:

$$S_{la} + S_{ga} = 1 \quad (7)$$

The VPL implementation on EWASG differs from that

available on the EOS4 module for water-air mixtures (Pruess, 1991), depending also on the choice of primary variables set. In EWASG the primary variables used for single phase conditions are total pressure of reference phase, P , salt mass fraction, $X^{(2)}$, NCG mass fraction, $X^{(3)}$, and temperature, T . If solid salt is present, the second primary variable is switched to solid saturation S_s . In two-phase conditions the third primary variable is switched from NCG mass fraction to gas phase saturation S_g .

The same primary variables set is used in EWASG with VPL capabilities in order to allow full compatibility with the previous version. VPL capabilities can be invoked simply by setting on/off a switch from the input deck.

In the presence of VPL effects due to suction pressure, the liquid phase can be present under conditions where vapor partial pressure and the gas phase total pressure are less than the brine saturation pressure. The thermophysical properties of liquid phase are calculated in these conditions considering the liquid phase pressure used by Pruess (1991):

$$P_l = \max(P_g, P_{b, \text{sat}}) \quad (8)$$

The liquid phase pressure determined with the above condition is also used to calculate the brine density for the Kelvin's equation.

CAPILLARY PRESSURE FUNCTION

Different geologic media show a great diversity of VPL and suction pressure relationships. Pruess and O'Sullivan (1992) presented a compilation of published experimental data with a description of available experimental methods.

Among the equations used to fit experimental data, Pruess and O'Sullivan considered for their numerical simulation study the equation suggested by van Genuchten (1980):

$$P_c = -P_0 (S_{ef}^{-1/\lambda} - 1)^{\lambda} \quad (9)$$

where:

$$S_{ef} = \frac{S_{la} - S_{lr}}{1 - S_{lr}} \quad (10)$$

P_0 , and λ are fitting parameters, whereas S_{la} is the active liquid saturation and S_{lr} is the liquid residual saturation. We used for our numerical studies the same capillary pressure curve used by Pruess and O'Sullivan with the following parameters obtained by Peters et al. (1984) through the fitting of experimental data obtained on tuff samples from Yucca Mountain:

$$S_{lr} = 0.0801$$

$$\lambda = 0.4438$$

$$P_o = 1.727 \text{ MPa}$$

Although the van Genuchten model allows consistent formulation for both capillary pressure and relative permeability functions, it presents the drawback that P_c goes to infinity as the liquid saturation approaches the residual value. The capillary pressure corresponding to the above parameters, is plotted vs the liquid phase saturation in Fig. 1. The figure also shows the VPL factor and the total pressure vs liquid saturation for a two-phase system at constant temperature of 220°C, for both pure water and a brine with a salt mass fraction of 20%.

As shown in Fig. 1, a maximum value of 500 MPa has been considered to avoid the infinity in the capillary pressure. Due to rapid increase of P_c at liquid saturation approaching the residual value, the VPL factor decreases from about 0.9 at $S_l=0.2$ to approx 0.1 at liquid saturation of 0.09. The effect of salt on VPL factor is limited: due to the higher liquid phase density, the VPL factor is slightly higher in the presence of saline brine. On the other hand, the total pressure is lower as the effect of VPL due to salinity prevails.

Fig. 1 suggests that, at least for selected capillary pressure curve, the effects of VPL due to suction will be important only at low liquid saturation values (Pruess and O'Sullivan, 1992).

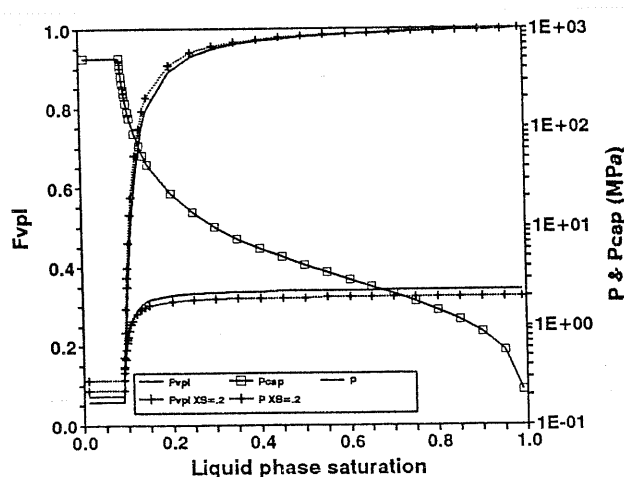


Fig.1 Capillary pressure, VPL factor and total pressure as a function of liquid saturation at a constant temperature of 220°C, for pure water and brine with 20% salt content.

DEPLETION OF TIGHT MATRIX BLOCKS

Most of the fluid reserves in vapor-dominated reservoirs are stored in tight matrix blocks with permeability in the order of microdarcy. Fracture systems are believed to contribute little to fluid storage, mainly providing large-scale permeability. The effect of VPL due to suction pressure is to generate an additional pressure decline as the block dries out, thus slowing down the recovery of fluid reserves.

Previous studies (Pruess and O'Sullivan, 1992) have analysed the effects of suction pressure on the depletion behaviour of tight matrix blocks, under conditions considered representative of vapor dominated systems. Battistelli et al. (1995) have examined the effects of salt content on depletion behaviour neglecting the VPL due to suction pressure. This paper presents simulations studies on the combined effects of permeability reduction and VPL due to salinity and suction pressure.

A model similar to that described by Pruess and O'Sullivan (1992) has been employed. It consists of a single block of rock matrix in the shape of a cube with side length of 50 m, which is to be viewed as a subdomain of a large reservoir volume. The block is surrounded by fractures with a small fractional volume of 10^{-4} . The matrix block is discretized according to the MINC method (Pruess and Narasimhan, 1985) with 15 nested cubes of 0.5%, 1%, 2%, 3%, 4%, 5%, 6%, 7%, 8%, 9%, 10%, 10%, 11%, 11%, and 12.5% volume fractions, as used by Battistelli et al. (1995). Matrix permeability, porosity density, specific heat and thermal conductivity are $5 \times 10^{-18} \text{ m}^2$, 5% , 2600 kg/m^3 , $920 \text{ J/kg}^\circ\text{C}$ and $2.51 \text{ W/m}^\circ\text{C}$, respectively.

The system is initially in two-phase conditions at temperature of 240 °C, with liquid saturation of 80% in the matrix block, and 1% in the fractures. Liquid relative permeability and capillary pressure are assumed in the van Genuchten form as used by Pruess and O'Sullivan (1992). Gas relative permeability is given by $k_{rg} = 1 - k_{rl}$. Block depletion occurs by a "well on deliverability" placed in the fractures with a prescribed wellbore pressure of 1 MPa, and a productivity index of $1.788 \times 10^{-13} \text{ m}^3$.

We modelled the permeability reduction using the series model for tubular flow with fractional length=0.8 and critical porosity fraction= 0.8. The equations employed have been presented by Battistelli et al. (1995) whereas a complete model description is given by Verma and Pruess (1988). Six cases are presented with different initial salt content. The effects of salt content and VPL on initial pressure and fluid reserves are summarized in Table 1.

Battistelli et al. (1995) found that in the depletion of low matrix permeability blocks persistent boiling near the block

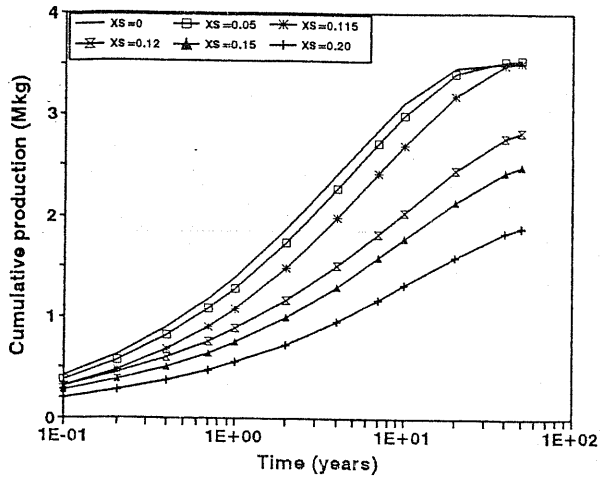


Fig. 2 Cumulative fluid recovery as a function of time for cases 1 to 6.

Case	Salinity (%)	Pressure (MPa)	Psat (MPa)	Mass in place (Mkg)	Water (Mkg)
1	0	3.323	3.348	4.088	4.088
2	5	3.221	3.244	4.306	4.092
3	11.5	3.066	3.086	4.585	4.060
4	12	3.052	3.073	4.607	4.056
5	15	2.970	2.989	4.736	4.028
6	20	2.821	2.839	4.948	3.962

Table 1. Initial pressure, saturation pressure and fluid reserves for different salt contents.

surfaces leads to concentration and, ultimately, precipitation of solids. They found that when the initial salt content is above a threshold value, the salt precipitation causes a severe loss in permeability so that the rate at which the fluid reserves are recovered is considerably lowered. For the same model used in this paper, neglecting the VPL due to suction pressure, the 'critical' salt mass fraction is between 0.08 and 0.085.

The effects of permeability reduction as a function of initial salt content in the presence of VPL effects due to suction pressure are presented in Fig. 2, which shows the cumulative mass production vs time for the 6 cases. It is interesting to note that the 'critical' initial salt mass fraction is increased to a value between 0.115 to 0.12. This increase is due to the fact that, avoiding complete vaporization of liquid phase inside the block, a higher value of salt mass fraction is necessary in order to reach the conditions for the sealing of block surfaces.

The change in behaviour below and above the threshold value is high-lighted in Fig. 3 showing the pressure distribution in the matrix block after 0.4 and 10 years.

At early times, 0.4 years, a high pressure decrease occurs near

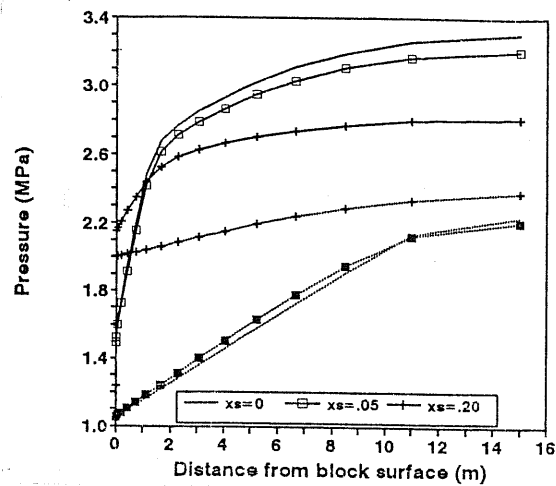


Fig. 3 Pressure distribution vs distance from block surface after 0.4 and 10 years for cases 1, 2 and 6.

the block surface due to low matrix permeability, producing strong vaporization. Since from the beginning no liquid phase is discharged from the block to the fractures being held by capillary forces, in the first matrix element salt accumulates owing to vaporization of brine flowing towards the block surface from the interior until salt precipitation takes place.

For initial salt content lower than the threshold value, the first matrix element vaporizes until the minimum value allowed by the VPL effects is approached, and the precipitation of solid salt starts in the second matrix element. Then vaporization takes place progressively in the interior of the block with precipitation of solid salt distributed in all the elements.

For initial salt content higher than the threshold value, the accumulation of salt in the first element is so fast that further boiling in this element is prevented. In fact the permeability reduction reduces the extracted mass rate and slows down the depletion associated processes. Consequently, all the matrix elements remain in two-phase conditions.

Fig. 4 shows liquid saturation as a function of distance from block surface at 10 years for cases 1, 2 and 6. Curves obtained with and without VPL due to suction pressure are compared. Below the threshold value (cases 1 and 2), the introduction of VPL avoids complete vaporization of the liquid phase. The liquid saturation close to block surfaces approaches the minimum value allowed by the capillary pressure curve chosen. Above the threshold value, the S_l distribution is almost identical, as for $S_l > 0.5$ the effect of VPL is very limited, as shown in Fig. 1 for the f_{VPL} factor as a function of liquid saturation.

As observed when VPL effects due to suction pressure are

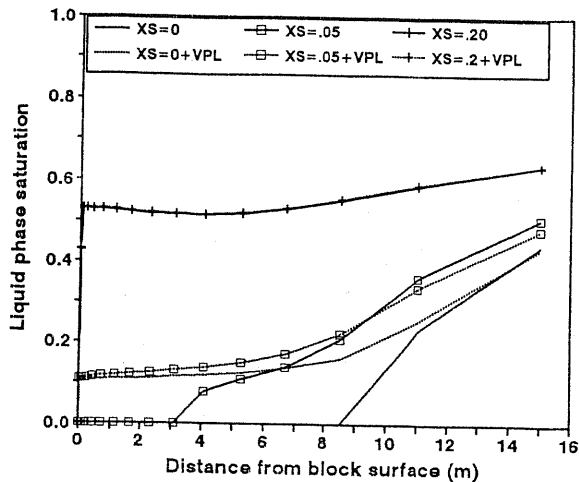


Fig. 4 Liquid saturation distribution vs distance from block surface after 10 years for cases 1, 2 and 6 with and without VPL due to suction pressure.

disregarded, two factors mainly control the depletion behaviour: boiling of the liquid phase with progressive drying out of matrix elements, and permeability reduction due to solid salt precipitation.

The change between the two observed behaviors depends on which factor prevails: at low salt content the first matrix element reaches the minimum liquid saturation value before the salt precipitation seals the matrix block surface.

To show how this process works, the pressure in the first matrix element is plotted as a function of time for all 6 cases in Fig. 5. At early time, the liquid saturation decreases faster for lower initial salt content because of higher extraction rate. For higher initial salt content the deposition of solid salt starts earlier and reduces the rate of pressure decline. When solid saturation approaches 0.20, the reduction of permeability is so high that production is strongly reduced and consequently the pressure becomes almost constant due to fluid redistribution in the interior of the block. For the cases shown, characterized by initial salt content far from the threshold value, the pressure history of first element with and without VPL effects due to suction is almost identical for the different cases. Total pressure is, of course, slightly smaller due to VPL effects.

The liquid saturation as a function of time is shown in Fig. 6 for the same cases with and without VPL effects. Whereas for $XS=0.20$ the history is almost identical, for cases below the threshold value the first element never vaporizes completely and a lower limit seems to be approached independently from the initial salt content.

The reasons for the convergence of liquid saturation at late

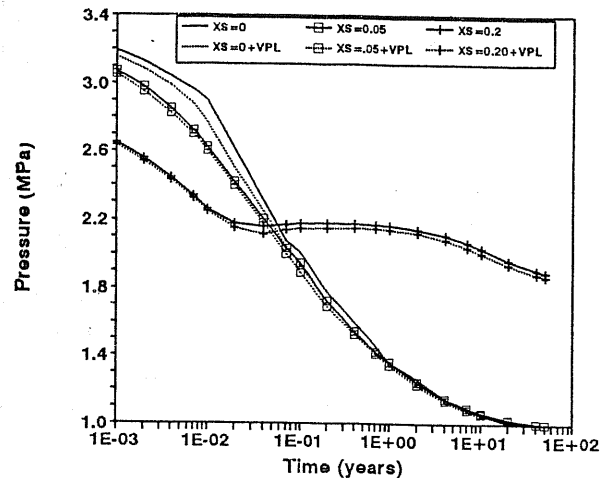


Fig. 5 Pressure history in the first matrix element for cases 1 to 6.

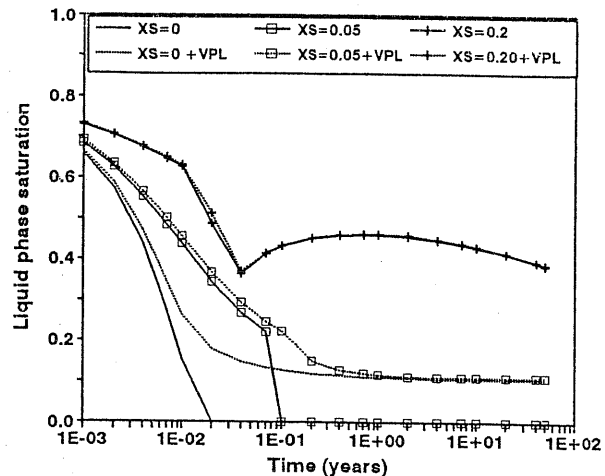


Fig. 6 Liquid phase saturation history in the first matrix element for cases 1, 2 and 6 with and without VPL due to suction pressure.

time towards a finite value independently from initial salt content lower than the threshold value, is due mainly to the shape of the adopted capillary pressure curve.

As the van Genuchten equation gives capillary pressure tending to infinity when the irreducible liquid saturation is approached, in our simulation the VPL factor decreases sharply when liquid saturation is lower than approximately 0.20. The well on deliverability option chosen for fluid extraction determines the minimum value for the pressure inside the block. At late time, close to 50 years, the pressure inside the block is almost 1 MPa everywhere for initial salt contents lower than the threshold value. Fig. 1 shows that the effect of salt on VPL due to suction pressure is very limited. Thus the total pressure of 1 MPa is reached at comparable S_1 values regardless of the initial salt content.

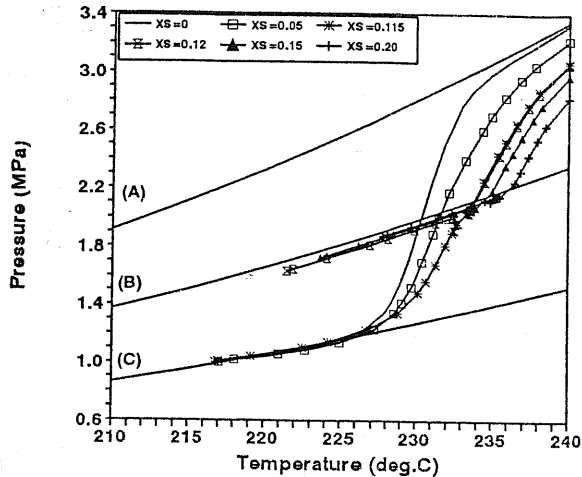


Fig.7 Thermodynamic path followed by the first matrix element during block depletion for cases E to I.

This behaviour does not change if a different value of irreducible liquid saturation is considered. Simulation runs for pure water utilising S_{lr} values of 0, 0.04 and 0.30 gave similar results. Different choices will naturally affect the threshold value at which the transition between the two different depletion behaviours occurs.

Similar results have also been obtained by using the same S_{lr} value and different P_o values equal to 50% and 200% of the value used in the base case. In this way the capillary pressure has the asymptotic behavior at the same S_l value and the curve is shifted down or up according to the increase or decrease of P_o parameter. The total pressure as a function of time changes, of course, according to the increase or decrease of VPL effects, but the depletion behaviour is almost identical.

The bottomhole pressure has also been changed from 1 MPa to 0.5 MPa. The recovery of fluid reserves was of course faster because of the higher pressure gradient, but it is interesting to note that the cumulative production after 50 years was only slightly higher. In fact, apart from the effects of minor differences in final block temperature, in order to reduce the total pressure to 0.5 MPa, a value of f_{VPL} equal to 50% of that of base case is necessary. For pure water, the final liquid saturation is about 9.6% instead of 10.6%. Thus the production increase, lowering bottomhole pressure to 50% of the initial base case value, corresponds to only 1% of liquid saturation.

Fig. 7 shows the thermodynamic path followed by the first matrix element during block depletion in terms of pressure vs temperature for all six cases. The saturation curve of pure water (A), that of NaCl saturated brine (B) and the saturation curve of pure water with VPL due to suction at a constant liquid

saturation of 0.106 (C) are also shown. It is evident that for cases 1, 2 and 3 (with initial salt content below the threshold value) the saturation curve of pure water with VPL effects at 10.6% liquid saturation is followed. The effects of salt on the VPL due to suction are limited.

On the other hand, the cases with an initial salt content above the threshold value (cases 4, 5 and 6) follow the shape of the brine saturation curve with NaCl concentration at saturation values.

CONCLUSIONS

The EWASG module including VPL due to salinity only and permeability reduction from the precipitation of salt, i.e. the EOS module for H_2O -NaCl- $NaCl$ mixtures developed for the TOUGH2 simulator by Battistelli et al. (1993, 1995), has been improved implementing the VPL due to suction pressure effects.

Simulation studies of fluid production from tight matrix blocks have been performed to evaluate the effects of VPL due to suction pressure on the depletion of fractured vapor-dominated reservoirs containing brines.

For the model and parameters investigated, previous simulations carried out using the EWASG module, showed a different depletion behavior depending on the initial NaCl concentration being higher or lower than a threshold value because of salt precipitation and related permeability reduction. The existence of these threshold values has been confirmed by simulation with VPL due to suction pressure effects included, but the change in the depletion behavior occurs at higher threshold values.

VPL due to suction pressure prevents complete dry-out of matrix block. Even for initial salt concentrations below the threshold value and after long production times, the block is in two-phase conditions and for the parameters used here, about 10% of initial water reserves are not produced.

Above the threshold value, persistent boiling near the surfaces of matrix blocks produces a severe loss in permeability, and considerably slows down the rates at which fluid reserves can be recovered. As liquid saturation remains at high values throughout the block, the VPL due to suction pressure does not produce remarkably effects.

Due to the strong dependence of the VPL factor from the relationship between suction pressure and liquid saturation, the results obtained are dependent upon the shape of capillary pressure function characteristics of different geologic media.

ACKNOWLEDGEMENTS

This work was supported by Aquater S.p.A. of the Italian National Hydrocarbons Agency (ENI), by the International Institute for Geothermal Research of the Italian National Research Council (CNR), and by the Assistant Secretary for Conservation and Renewable Energy, Geothermal Division, of the U.S. Department of Energy under contract No DE-AC03-76SF00098.

NOMENCLATURE

$F(k)$	mass flux of component k , $\text{kg}/(\text{s m}^2)$
f_{vpl}	vapor pressure lowering factor, dimensionless
g	acceleration of gravity, m^2/s
k	intrinsic permeability, m^2
k_{β}	relative permeability to β phase
$M^{(k)}$	accumulation term of component k , kg/m^3
n	unit normal vector
P	pressure, Pa
P_c	capillary pressure, Pa
P_o	fitting parameter in the van Genuchten's equation
$Q^{(k)}$	source term for component k , $\text{kg}/(\text{s m}^3)$
R	universal gas constant, $8,314 \text{ J}/^\circ\text{C mole}$
S_{β}	saturation of phase β
T	temperature, $^\circ\text{C}$
V_n	volume of grid element n , m^3
$X^{(k)}$	mass fraction of component k
$W^{(k)}$	molecular weight of component k , kg/mole
Γ_n	surface area of grid element n , m^2
ϕ	porosity
λ	fitting parameter in the van Genuchten's equation
μ	dynamic viscosity, Pa s
ρ	density, kg/m^3

Subscripts and Superscripts

a	active
b	brine
g	gas phase
l	liquid phase
r	residual
s	solid salt phase
sat	vapor-saturated
1	water component, H_2O
2	salt component, NaCl
3	gas component, NCG
β	phase index

REFERENCES

- Battistelli, A., Calore, C. and Pruess, K. (1993). *A Fluid Property Module for the TOUGH2 Simulator for Saline Brines with Non-Condensable Gas*. Proc. 18th Workshop on Geoth. Res. Eng., Stanford University.
- Battistelli, A., Calore, C. and Pruess, K. (1995). *Analysis of Salt Effects on the Depletion of Fractured Reservoir Blocks*. Proc. World Geoth. Congress, Florence, May 18-30, in press.
- Nghiem, C. P., and Ramey, H. J. Jr. (1991). *One-Dimensional Steam Flow in Porous Media under Desorption*. 16th Workshop on Geoth. Res. Eng., Stanford University.
- Peters, R. R., Klavetter, E. A., Hall, I. J., Blair, S. C., Heller, P. R., and Gee, G. W. (1984). *Fracture and Matrix Hydrologic Characteristics of Tuffaceous Materials from Yucca Mountain, Nye County, Nevada*. Sandia Ntl. Lab., Report SAND84-1472.
- Pruess, K. and Narashiman, T. N. (1985). *A Practical Method for Modeling Fluid and Heat Flow in Fractured Porous Media*. Soc. Pet. Eng. J., Vol. 25(1), pp. 14-26.
- Pruess, K. (1991). *TOUGH2 - A General-Purpose Numerical Simulator for Multi-phase Fluid and Heat Flow*. Earth Sci. Div., Lawrence Berkeley Laboratory Report LBL-29400.
- Pruess, K. and O'Sullivan, M. (1992). *Effects of Capillarity and Vapor Adsorption in the Depletion of Vapor-Dominated Geothermal Reservoirs*. Proc. 17th Workshop on Geoth. Res. Eng., Stanford University.
- Verma, A. and Pruess, K. (1988). *Thermohydrological Conditions and Silica Redistribution Near High-Level Nuclear Wastes Emplaced in Saturated Geological Formations*. J. of Geophys. Res., Vol. 93(B2), pp. 1159-1173.